Positron mobility in perylene

A. P. Mills, Jr.
AT&T Bell Laboratories, Murray Hill, New Jersey 07974

N. Karl
3. Physikalisches Institut, Universität Stuttgart, D-7000 Stuttgart 80, Germany
(Received 11 December 1992)

Based on Doppler-shift measurements we have determined the positron drift velocity u in a high-purity monoclinic α-perylene single crystal as a function of applied electric field F and temperature. The electric field is applied as a triangular wave with a maximum field F_{max}. At low fields the drift velocity displays a linear field dependence, while it assumes a sublinear field dependence above a characteristic velocity $v_s = 50$ km/s and finally tends to saturate at 110 km/s, presumably due to optical-phonon generation above a certain threshold kinetic energy. Unlike in the case of diamond, v_s is much greater than the longitudinal sound velocity in the solid. By fitting the observed nonlinear electric-field dependence of u to a Shockley expression for acoustic deformation potential scattering of "warm" charge carriers we extract the zero-field limit of the positron mobility μ_0 along the crystallographic c' axis ($c' \| a \times b$). At 297 K $\mu_0 = (136 \pm 3 \pm 14)$ cm^2 V^{-1} s^{-1}, where the first error is statistical and the second is an estimated $\pm 10\%$ calibration uncertainty. Over the temperature range 100–350 K the mobility exhibits a T^n temperature dependence with $n = -1.04 \pm 0.03$, showing a clear departure from the $T^{-3/2}$ dependence one might expect. Below 100 K μ_0 still increases with decreasing temperature, but at a given temperature its value decreases as the maximum applied field F_{max} increases, possibly indicating interference caused by the presence of a field-enhanced accumulation of trapped carriers that cause scattering at low temperatures. Below 50 K the limit of μ_0 as $F_{max} \to 0$ does not further increase but reaches a maximum value of ≈ 1000 cm^2 V^{-1} s^{-1}, an upper limit which is presumably set by the presence of residual impurities. These data will be compared with positron mobility results obtained for anthracene.

I. INTRODUCTION

Positrons are widely used to study the electronic properties of various solids. Because of the great propensity of positrons for finding trapping sites,[1,2] it is important to learn about positron states and diffusion mechanisms in order to distinguish intrinsic properties from those caused by defects.[3] Mobility measurements can tell us whether a particle moves by hopping or by propagation in a band and whether scattering from impurities or phonons is dominant. Single-crystal samples of organic molecules can be prepared with high purity[4–6] such that we should be able to discern the nature of the intrinsic scattering mechanisms. Nonpolar solids are expected to have a small acoustic-phonon coupling for positrons and therefore should display a large positron mobility. We have found that anthracene, a nonpolar aromatic hydrocarbon molecule consisting of three condensed benzene rings [see molecular structure symbols in Fig. 6(b)], has a large mobility for positrons. We concluded that the positrons exist as delocalized Bloch states in the solid.[7] Unfortunately, we were unable to follow the mobility to low temperatures because of a degradation of the sample with time. As we shall show below, the mobility recovers upon warming, but the conclusions are slightly ambiguous. Perylene [for the molecular structure, see Fig. 6(a)] is a related five-ringed aromatic hydrocarbon that we were able to study without problems down to temperatures as low as 100 K. We find that the positron mobility in perylene increases substantially with decreasing temperature, reaching 1000 cm^2 V^{-1} s^{-1} at 50 K.

For convenience, we recall some relevant information about charge-carrier mobilities. At low electric fields, the drift velocity u of an electron, hole, or positron in a solid should be linearly related to the applied electric field F,

$$u = \mu_0 F \ , \tag{1}$$

where μ_0 is the zero-field limit of the mobility. The average drift velocity of the positrons annihilating in a solid may be determined from the Doppler shift $\Delta E/E = u/2c$ of the annihilation photons in the direction of F.[8] If positrons behave analogously to electrons and holes in semiconductors,[9] the acoustic-phonon-limited positron mobility for a crystal of cubic symmetry would be given by

$$\mu_0 = [(8\pi)^{1/2}/3] v_l^2 \hbar^4 \rho m^{-5/2} e \varepsilon_d^{-2} (mT)^{-3/2} \ , \tag{2}$$

where ρ is the density of the solid, m is the positron effective mass, ε_d is the deformation potential constant characterizing the positron-phonon coupling, and v_l is the longitudinal sound velocity. At high electric fields, a sublinear field dependence of the drift velocity u of "warm" charge carriers, no longer in thermal equilibrium with the crystal lattice, is predicted by Shockley's expression for the acoustic-phonon-limited drift velocity of a nondegenerate particle,[10]

$$u(F) = 2^{1/2} \mu_0 F \{1 + [1 + (3\pi/8)(\mu_0 F / v_s)^2]^{1/2}\}^{-1/2} \ , \tag{3}$$

0163-1829/93/48(10)/7050(7)/$06.00

where μ_0 is the low-field mobility. Such a sublinear field dependence of the electron and hole drift velocity is indeed well known for inorganic semiconductors and has recently also been found for organic photoconductors (cf. Ref. 4). In addition, at very high applied fields a tendency to velocity saturation not contained in Eq. (3) can exist, caused by the collisional emission of optical phonons, a process that becomes possible as soon as the kinetic energy of the charge carrier exceeds the threshold energy for optical-phonon generation.[11,12] To extract the low-field mobility μ_0 and the characteristic velocity v_s by curve fitting, we shall assume that the functional form of Eq. (3) is correct for not too large drift velocities. As noted by Ryder and Shockley,[13] the characteristic velocity v_s to be used in Eq. (3) may deviate from the longitudinal sound velocity v_l originally introduced by the model. Whereas in diamond $v_s = v_l$,[14] we find that a value $v_s \approx 50$ km/s much higher than v_l describes the observed onset of the nonlinearity of the drift velocity in perylene.

Our sample is a single slab of material irradiated from one side by a positron source. The reason for using an asymmetric geometry rather than a symmetric two-slice sandwich structure is that a significant portion of the positrons can drift to the surface of the sample under the influence of the electric field. At the surface and in other inert portions of the material surrounding the radioactive source, the positrons do not have a net drift velocity. Annihilation photons from such effectively stationary positrons are detected along with those from the positrons moving in the sample and must be taken into account. With the field direction (positive) causing the positrons to drift into the sample away from the surface, there is no surface-related reduction of the Doppler-effect signal. The apparent measured drift velocity will thus be

$$v_d = u(F)[1 - L(u)] , \tag{4}$$

where $L(u)$ is the fraction of the positrons implanted into the sample that find their way to the surface. The shift of order 1 eV in the mean annihilation γ-ray energy due to the different potentials and electrons sampled by the mobile and nonmobile positrons makes a second-order correction to Eq. (4) for negative field directions, but will not affect our determination of the positron mobility that relies primarily on the positive field direction data. In Eq. (4) we are assuming that the measured drift velocities have already been corrected by dividing the raw measured drift velocity by ζ, the fraction of the positrons that stop in the sample. For a beta emitter source in contact with a flat sample, the probability for a positron emitted toward the sample to be stopped at a penetration depth x is

$$P(x) = \beta \int_0^{\pi/2} e^{-x\beta/\cos\theta} \tan\theta \, d\theta = \beta \int_0^1 e^{-x\beta/y} dy/y , \tag{5}$$

where β^{-1} is the exponential attenuation length for the beta particles. The fraction of the implanted particles reaching the surface as a function of their inverse diffusion length ξ is

$$L(\xi) = \int_0^\infty P(x) e^{-\xi x} dx = \beta \xi^{-1} \ln(1 + \beta^{-1}\xi) , \tag{6}$$

where ξ is given by a superposition of the thermal and the field-induced motion,[15]

$$\xi = \frac{u}{2D} + \left\{ \left[\frac{u}{2D} \right]^2 + \frac{1}{D\tau} \right\}^{1/2} . \tag{7}$$

Here τ is the positron lifetime in the sample and D is the diffusion coefficient related to the mobility by the Nernst-Einstein relation $D = \mu_0 kT/e$.

II. EXPERIMENT

Our data were obtained in the same manner as in previous experiments on polyethylene,[16] anthracene,[7] and diamond.[14] The method is based on the fact that an annihilation of a positron of velocity $\mathbf{v}$ with an electron of zero average momentum leads to an average Doppler shift of the energy of the annihilation quanta,

$$\Delta E/E \approx \tfrac{1}{2} \mathbf{v} \cdot \hat{\mathbf{n}}/c , \tag{8}$$

where $\hat{\mathbf{n}}$ is a unit vector in the direction of the detector and where the factor of $\frac{1}{2}$ is caused by the fact that the electron is at rest on average. The energy of the 511-keV annihilation photons was measured with an intrinsic Ge detector (35% efficiency) having a 1.65-keV resolution and a 29.5% photofraction at 514 keV. The pulses from the detector were amplified, shaped with a 1.5-μs time constant, and sent to a three-level, two-window pulse-height analyzer made by modifying an Ortec model 551 single-channel analyzer. The energy windows A and B from the latter were about 2 keV wide and were set on the lower and upper halves of the 511-keV photopeak, respectively. The lower level of B was determined by the same threshold detector that determined the upper level of A. The amplifier gain was adjusted automatically and continuously by a long-time-constant (> 100 s) feedback loop that sensed the difference in the A and B count rates. The average count rates were thus kept equal without affecting the sensitivity to instantaneous changes due to the positron drift in the applied electric field. The two rates A and B were recorded simultaneously in two 1024-channel data fields of a 4-input 4096-channel multiscalar. The channel number at which the counts were added swept continuously up and down with a 0.5–4-ms dwell time at each channel. An analog voltage corresponding to the channel number was amplified to produce a symmetric sawtooth wave V_1 and its inverse V_2 with maximum amplitudes $\pm V_{\max}$ that were applied to the two sides of the sample to produce the drift field F.

A Doppler shift of the 511-keV annihilation photons causes equal and opposite changes in the count rates A and B. The instrument was calibrated by turning off the gain control feedback loop, introducing changes $\Delta G/G$ in the amplifier gain G and noting the corresponding changes ΔN in the count rates A and B. The gain changes were made by adding or subtracting 0.320-Ω resistors in series with the 34-Ω output impedance of the amplifier. Using the measured 758-Ω input impedance of the two-window pulse-height analyzer, we calculate that the gain changes were $\Delta G/G = \pm 4.04 \times 10^{-4}$. The positron drift velocity at a particular value of the electric field F is computed from the count rates $N_A(F)$ and $N_B(F)$ using Eq. (8) ($v_d = 2c\,\Delta E/E$) and the expression

$$\Delta E/E=\tfrac{1}{2}[\Delta N_A(F)/\langle N_A\rangle-\Delta N_B(F)/\langle N_B\rangle]\alpha^{-1}\ , \quad (9)$$

where the proportionality constant

$$\alpha=\zeta\frac{\partial \ln N}{\partial \ln G}=\zeta\frac{\Delta N/N}{\Delta G/G}$$

is the relative count rate change per induced gain change. In Eq. (9), $\langle N_i\rangle$ is the average number of counts and $\Delta N_i(F)=N_i(F)-\langle N_i\rangle$. The value of the constant determined from measurements of ΔN vs ΔG was $\alpha=88.8\pm1.6$, including the factor $\zeta=0.5$ to account for the fact that roughly half of the positrons annihilate in the material of the source and cold finger, hence diluting the Doppler-shift signal. [It is obvious from Eq. (9) that symmetrically increasing the count rates $\langle N_i\rangle$ by a factor of, e.g., 2 in both windows A and B by addition of an equal number of non-Doppler-shifted pulses leads to an apparent drift velocity which is half the true one as long as $\Delta N \ll N$.] The value of α was found to be constant to within better than 2% over the 100-day duration of the experiment. We make no correction for positronium formation. We assume that positronium does not form in perylene, since it does not form in its close relative anthracene.[17] The computed electric field $F=(V_1-V_2)/\Delta x$ is the applied voltage difference divided by the sample thickness Δx.

The sample slice 0.71 mm thick oriented with the c' direction perpendicular to the face of the slice was cut from a single-crystal boule of zone-refined perylene (crystal number K677) by using a xylene-wetted cotton thread on a "wire" saw. A source of 20 μCi of ^{22}Na was deposited on a Cu block in thermal contact with but electrically isolated from the end of a closed-cycle refrigerator cold finger. The source was covered with a 5-μm Mylar film.[18] The perylene sample was placed over the source, covered by an Al plate and held in place by a 304 stainless-steel spring. The two voltages V_1 and V_2 were applied to wires connected to the Cu block and to the spring, respectively. The electric field F was thus applied perpendicular to the face of the sample slice, i.e., in the c' direction. As is shown in Fig. 1, the source was located on the axis of the cylindrical 57-mm-diam×60-mm-long Ge detector crystal, approximately 75 mm from its face. To correct our Doppler-shift measurements for the average value of $1/\cos\theta$, all results reported here should be multiplied by 1.05. On the other hand, the fraction ζ of the positrons from the source that stop in the sample is decreased by several percent as a result of attenuation in the Mylar foil and is uncertain by several percent as a result of the different amount of backscattering from the Cu cold finger and the sample. We shall take account of these unknown factors and the solid-angle factor into a $\pm10\%$ systematic uncertainty estimate.

The sample temperature was measured with a Si diode (A) attached to the sapphire insulator shown in Fig. 1. The temperature was held constant within ±0.1 K at a particular setting between 14 and 350 K by feedback to the sample heater. After the experiment was completed, a second Si diode (B) calibrated to better than ±0.5 K for 2–100 K and ±1 K for 100–300 K was attached to the Cu sample stage less than 10 mm from the sample. The readings of the two diodes were compared over the range 17–300 K. We found that within ±0.2 K the two readings are related by the expression

$$T_B=0.9955T_A-0.2\ \text{K}\ , \quad (10)$$

which amounts to a 1.4-K difference at room temperature. We use Eq. (10) to correct the sample temperatures T_A recorded during the mobility runs.

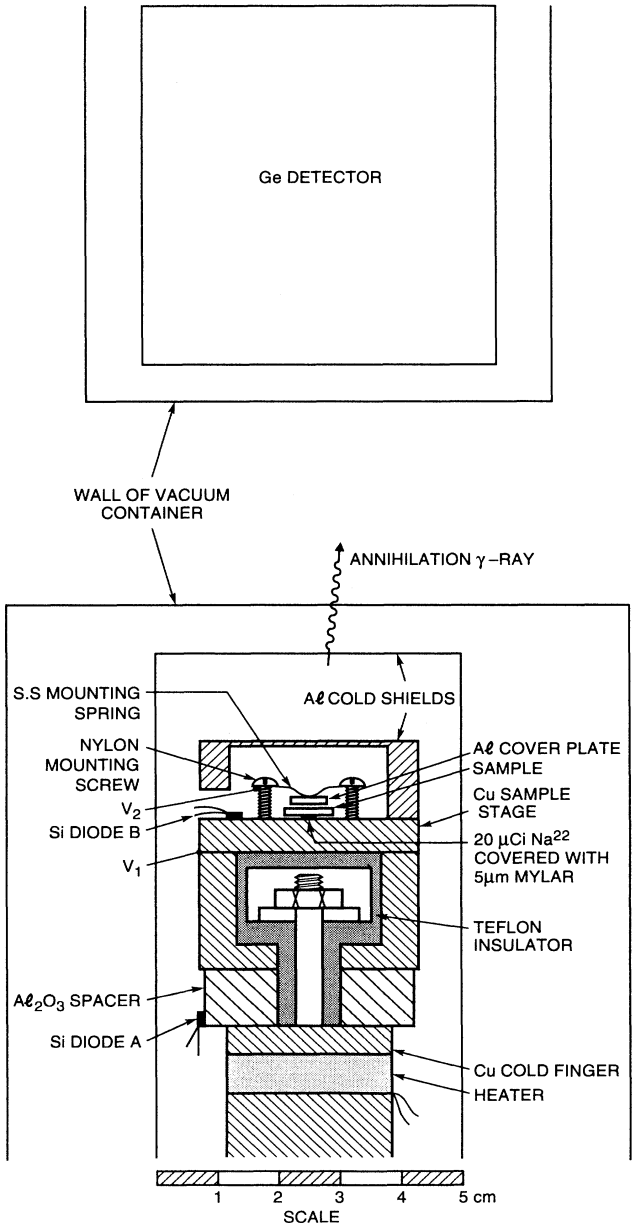

FIG. 1. Schematic view of the sample and detector. Si diode B was mounted at the end of the experiment to calibrate the temperature reading of Si diode A.

III. RESULTS

Figure 2 shows the positron drift velocity v_d in the high-purity perylene single crystal as a function of applied electric field F for four temperatures. Our complete data set was obtained during approximately 95 one-day runs at 36 temperatures. Reversal of the voltage leads caused no observable change in our measurements except for the sign. There is also no difference in measurements made at different dwell times per channel of 0.5–4.0 ms. The data were fitted by the method of least squares using Eqs. (3)–(7). Because the data are not symmetric about $F=0$, as expected from Eq. (4), whereas the procedure of Eq. (9) artificially causes the average value $\langle v_d \rangle = 0$, we have included in the fit a drift-velocity offset parameter b for each run. For plotting purposes we have subtracted the offset b from the data so that the expected value of v_d is zero for $F=0$. To extract the zero-field limit of the positron mobility μ_0 without biasing the result due to possible inadequacies of the model for the effect of positron loss at the surface, we restricted the range of the fit to include only the lowest five points for negative values of F. Drift velocities greater than 60 km s^{-1} were not used in the fit because of the inadequacy of Eq. (3) in

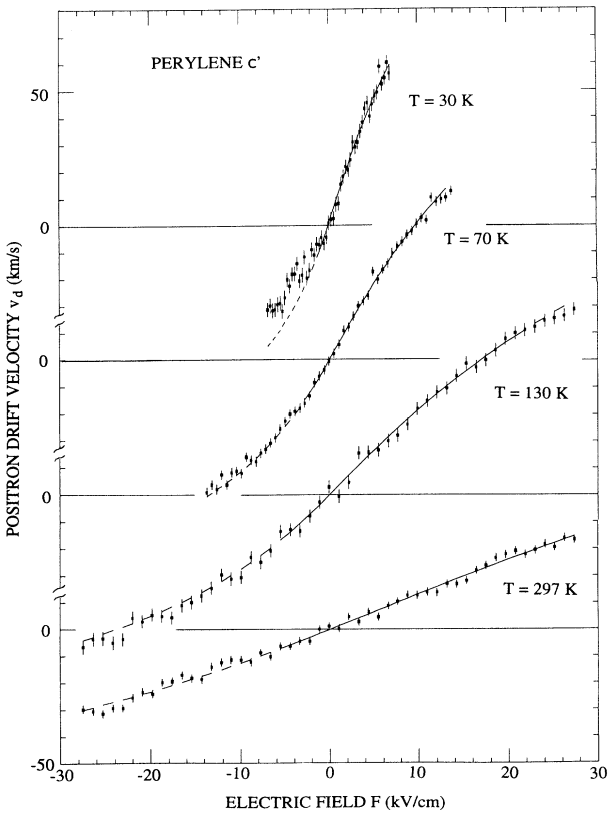

FIG. 2. Positron drift-velocity measurements vs applied electric field in a single crystal of high-purity (monoclinic) α-perylene oriented with the c' direction parallel to the electric field F. The solid curves are fitted expressions [see text and Eq. (3)] for the drift velocity that are used to determine the low-field limit of the positron mobility. The dashed portions of the curves are continuations beyond the range of F used for the fit.

TABLE I. Low-electric-field positron mobilities μ_0 in perylene at various sample temperatures T and for different values of the maximum applied voltage V_{max}. The parameter b is the drift-velocity offset parameter. The values in parentheses are one-standard-deviation error estimates; χ^2 is the value of chi squared, and N is the number of degrees of freedom for the model fit to the data for each run.

V_{max} (V)	T (K)	μ_0 (cm^2 V^{-1} s^{-1})	b (km s^{-1})	χ^2	N
500	14	830(12)	−0.3(0.4)	40.71	26
2000	14	614(24)	0.2(1.0)	20.12	11
250	17	753(57)	−1.2(1.0)	33.90	26
500	17	871(32)	1.8(0.9)	41.90	26
2000	17	631(14)	−1.5(0.6)	9.81	11
500	20	912(16)	−0.6(0.5)	22.71	26
500	25	892(27)	−1.0(0.8)	30.10	26
2000	25	690(21)	−0.7(0.9)	17.90	12
4000	25	504(8)	−1.2(0.4)	9.53	7
500	30	1020(30)	0.9(0.8)	30.53	26
250	35	900(44)	0.5(0.7)	32.39	26
500	40	895(27)	0.8(0.8)	28.12	26
500	45	841(32)	0.3(0.9)	35.78	26
250	50	732(25)	−0.5(0.4)	38.04	26
500	50	778(15)	0.3(0.4)	21.90	26
1000	50	679(10)	−0.3(0.4)	14.59	21
2000	50	721(23)	−1.3(0.9)	26.39	10
500	55	734(29)	0.5(0.9)	35.59	26
500	60	680(26)	−1.3(0.8)	36.95	26
500	65	592(24)	0.0(0.8)	30.40	26
1000	70	594(9)	−0.3(0.5)	21.02	24
250	75	539(24)	0.1(0.4)	48.39	26
500	75	559(16)	−0.1(0.5)	27.35	26
1000	75	544(16)	1.1(0.8)	30.18	24
2000	75	490(16)	−1.5(0.9)	21.81	15
1000	80	533(17)	−0.3(0.9)	36.47	26
500	90	514(28)	−0.5(0.9)	43.32	26
2000	100	444(13)	−0.1(0.8)	20.62	17
1000	110	398(13)	−1.3(0.8)	34.57	26
250	120	332(22)	0.1(0.4)	25.46	26
500	120	357(21)	0.7(0.7)	28.92	26
1000	120	348(9)	−0.5(0.5)	29.68	26
2000	120	348(12)	−0.8(1.0)	32.50	20
2000	130	337(8)	−0.1(0.7)	18.79	20
1000	140	312(14)	−0.3(0.9)	39.84	26
2000	150	309(14)	0.2(1.3)	37.62	23
2000	160	270(8)	−0.2(0.8)	34.13	26
2000	170	245(7)	−0.9(0.8)	27.53	26
2000	180	239(7)	−1.4(0.8)	30.68	26
2000	190	227(7)	0.5(0.8)	36.94	26
2000	200	210(5)	−0.6(0.6)	36.38	26
2000	210	213(4)	−0.5(0.4)	18.93	26
2000	225	201(3)	0.1(0.3)	13.81	26
2000	240	180(5)	−1.1(0.6)	27.70	26
2000	250	163(4)	0.5(0.4)	20.78	26
2000	275	149(5)	−1.7(0.6)	35.60	26
2000	297	136(3)	−0.1(0.4)	27.52	26
4000	297	141(2)	−0.2(0.4)	12.52	23
2000	300	139(7)	1.1(0.9)	33.38	26
2000	325	126(3)	−0.4(0.4)	27.89	26
2000	350	114(4)	0.8(0.5)	32.44	26

describing the high-field saturation effect indicated in Fig. 2 and more clearly evident at lower temperatures (Fig. 3). Fixing the positron lifetime τ of Eq. (6) to be 300 ps,[19] the exponential attenuation coefficient of Eq. (5) and the parameter v_s of Eq. (3) that gave the best fit to the entire data set were $\beta^{-1}=43\pm10$ cm^{-1} and $v_s=49\pm2$ km s^{-1}. The value of β^{-1} is in agreement with the 44 cm^{-1} obtained from the mass-absorption coefficient for beta particles from ^{22}Na having a 0.54-MeV end-point energy,[20] 33 cm^2 g^{-1}, and using as the density of perylene 1.332 g cm^{-3}. Unlike the case of diamond,[14] v_s is much greater than the longitudinal sound velocity in the solid, v_l. The solid lines in Fig. 2 show the fitted curves from Eqs. (3)–(7), and the dashed lines show the extension of the curves beyond the fitted region. Table I is a list of the maximum applied voltage, the fitted zero-field mobility μ_0, the drift velocity offset b, and the Chisquare per degree of freedom N for each sample temperature. Several 1-day runs are typically included at each temperature. The fits are typically quite good and match the data even for large negative F in most cases.

At very low temperatures, as shown for example in Fig. 3, we note that the zero-field mobility becomes less

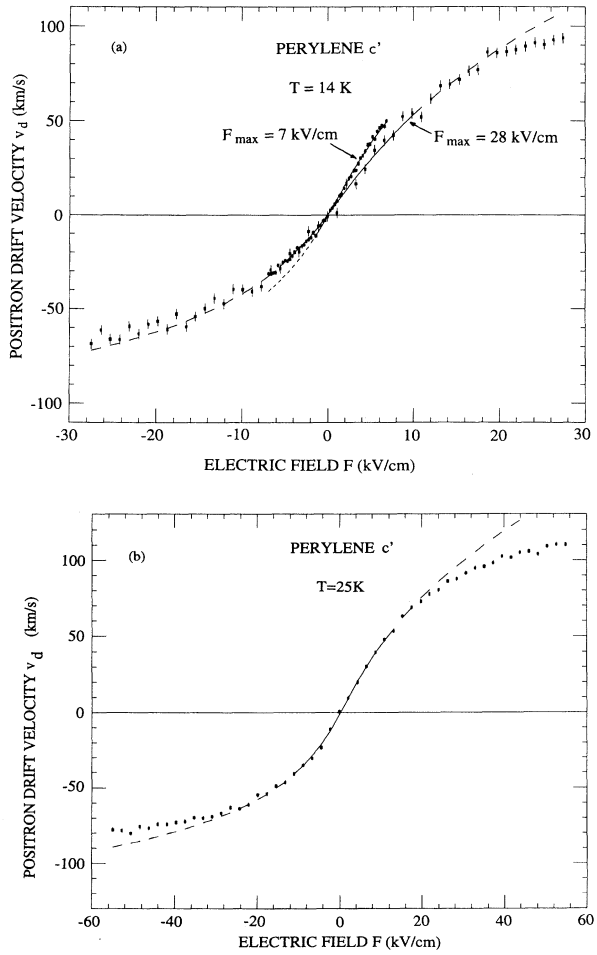

FIG. 3. Positron drift velocity vs electric field for two different ranges of the periodically swept applied field F at $T=14$ K and for 25 K. The curves are fitted as in Fig. 2.

when the range of the applied electric field, $\pm F_{\max}$, is further extended. Let us assume that the effect is linear in $F_{\max}$, the maximum applied field,

$$\mu_0(F_{\max})=\mu_0(F_{\max}\to0)+\left[\frac{\partial\mu_0}{\partial F_{\max}}\right]F_{\max}\ . \tag{11}$$

Least-squares fitting of the data at the seven temperatures for which several values of $F_{\max}$ were used, we find the parameters given in Table II. Figure 4 is a plot of the parameter $\partial\mu_0/\partial F_{\max}$ vs sample temperature. The data are consistent with the hypothesis that above 100 K there is no effect on the low-field mobility associated with large values of the applied electric field ($\partial\mu_0/\partial F_{\max}=0$), whereas below 100 K the slope $\partial\mu_0/\partial F_{\max}$ is nonzero. It is approximately linear in T,

$$\frac{\partial\mu_0}{\partial F_{\max}}=a+bT\ . \tag{12}$$

A least-squares fit yields $b=0.11\pm0.02$ and $a=-10.5\pm0.9$.

Another low-temperature effect was noticed in our experiment on *anthracene*, namely, that the positron mobility decreased with time. Figure 5 shows the mobility of positrons in a high-purity c'-oriented anthracene sample at temperatures between 50 and 68 K as a function of the time since cooling below 150 K. The decay of μ_0 is evidently a nonexponential function of time. No such effect was observed in our experiment on perylene. In a 6-day run at 14 K, the decay of the mobility was found to be $(0.3\pm0.8)\%$ per day, consistent with zero and much smaller than the roughly 30% per day effect in Fig. 5 for anthracene.

In Fig. 6(a) we present our measurements of the low-field positron mobility for perylene. The data are from Table I and have been extrapolated to zero *maximum*

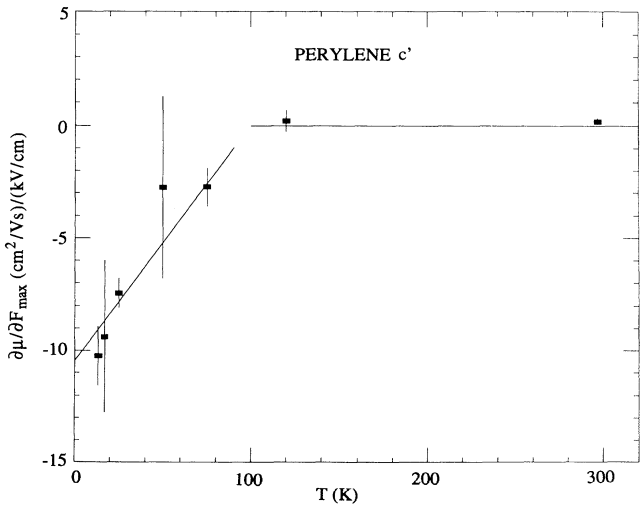

FIG. 4. Derivative of the extrapolated zero-field positron mobility with respect to the maximum value of the applied electric field F vs temperature T. The two line segments are the fitted linear dependence of $\partial\mu/\partial F_{\max}$ for T less than 100 K and the assumed zero value of $\partial\mu/\partial F_{\max}$ for T greater than 100 K.

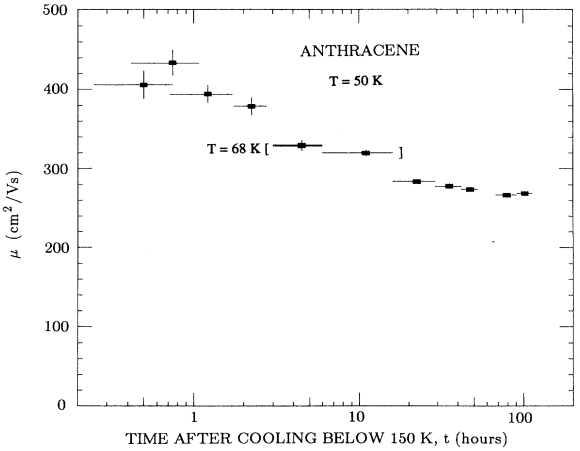

FIG. 5. Time dependence of the positron mobility $\mu_{c'c'}$ in high-purity anthracene following cooling below 150 K. For these runs, $F_{max} = 19$ kV cm^{-1}.

TABLE II. Derivative with respect to the maximum applied electric field F_{max} of the low-electric-field positron mobility μ_0 in perylene at various sample temperatures T, $\partial\mu_0/\partial F_{max}$, and zero-maximum-electric-field extrapolation of the mobility, $\mu_0(F_{max} \to 0)$. The values in parentheses are one-standard-deviation error estimates; χ^2 is the value of chi squared, and N is the number of degrees of freedom for a linear fit to the data for each run.

T (K)	$\partial\mu_0/\partial F_{max}$ [(cm^2 V^{-1} s^{-1})/(kV cm^{-1})]	$\mu_0(F_{max} \to 0)$ (cm^2 V^{-1} s^{-1})	χ^2	N
14	−10.2(1.3)	902(18)	0.00	0
17	−9.4(3.3)	897(83)	5.37	1
25	−7.5(0.7)	923(34)	1.85	1
50	−2.9(4.1)	750(59)	24.86	2
75	−2.8(0.8)	573(15)	1.63	2
120	0.2(0.5)	345(9)	0.67	2
297	0.2(0.1)	131(6)	0.00	0

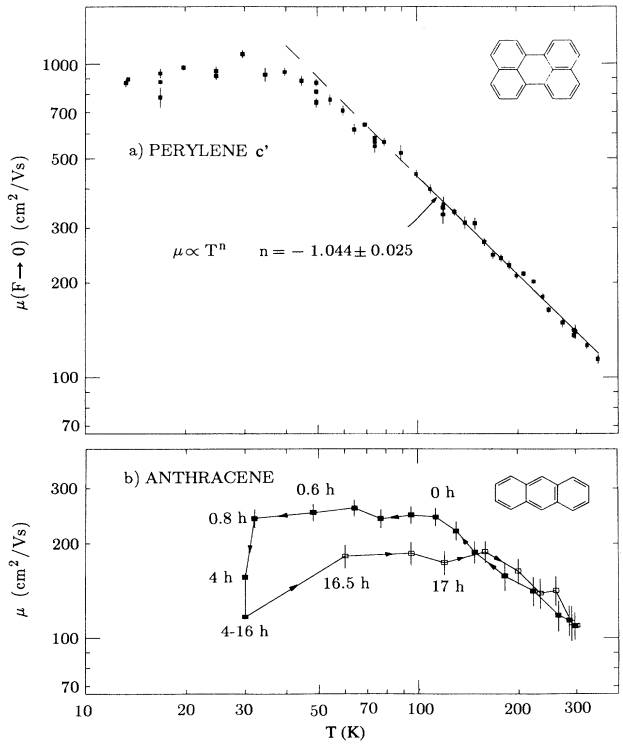

FIG. 6. (a) Zero-field limit of the $c'c'$ component of the positron mobility μ_0 in perylene. The data for T less than 100 K have been corrected for the effect of the maximum applied electric field using the slope determined in Fig. 4. (b) Positron mobility $\mu_{c'c'}$ in less pure anthracene than in Fig. 5. The data were obtained during rapid cooling down to 30 K, at which temperature the mobility displayed a decrease with time. The mobility partially recovered upon warming to 60 K and fully recovered its initial value upon warming above 150 K. The chemical structures of the molecules are shown.

electric field using Eqs. (11) and (12) for T less than 100 K, a procedure unnecessary for the $T > 100$ K data. The data for T greater than 100 K have then been fitted by a power law $\mu \propto T^n$, with the result $n = -1.04 \pm 0.03$. For comparison, Fig. 6(b) shows our measurements on an anthracene sample of lesser purity than that of Fig. 5. A strong decrease of μ_0 with time is observed, although the measurements were made rapidly to avoid the decay effect as much as possible. It appears that the positron mobility recovers partially upon warming to 60 K and fully upon warming to 150 K. In the higher-temperature range from 150 to 300 K where data obtained upon cooling and warming up are fairly coincident, the temperature dependence, as in perylene, is consistent with a T^{-1} behavior.

IV. DISCUSSION

The non-$T^{-3/2}$ temperature dependence of the positron mobility in perylene, the saturation drift velocity much greater than the sound velocity, and the effective reduction of the low-field mobilities after the application of large electric fields at very low temperatures are all unusual. The existence of a more complicated temperature dependence than the predictions of Eq. (1) is not new since it is known that the *electron* mobility varies as T^n with $n = -1.78$, -1.69, and -2.16 with the electric field parallel to the a, b, and c' directions.[21] Given that the positron is at the bottom of the lowest band and is unrestricted by the Pauli exclusion principle, we have a situation of unusual simplicity. It might therefore be possible to construct a sufficiently accurate theoretical model to explain the exponent $n = -1$ and why the appropriate velocity to use in Eq. (3) is more than an order of magnitude greater than the longitudinal sound velocity. The largest positron drift velocity attained in perylene, 10^7 cm s^{-1}, is about 4 times greater than that measured for electrons.[21] This observation may tentatively be ascribed to a positron effective mass for the c' direction of about $1m_e$, much less than that of electrons in the conduction band of perylene for the same field direction (cf. Ref. 4).

We would here be assuming that the cause for the observed velocity saturation at the highest electric fields applied is the same for electrons and for positrons, namely, the generation of optical phonons by fully inelastic collisions with the crystal lattice as soon as the particle kinetic energy is just high enough.[12] The effect of a pretreatment by large instantaneous electric fields on the low-field mobility possibly indicates the presence of a field-enhanced accumulation of trapped electrons or holes that cause scattering at low temperatures. Whether a similar effect might be present in the electron and hole mobility measurements is an interesting question. The latter are performed with pulsed currents of the order of 100 μA, which are far greater than the positron currents, even if one includes ionization caused by the stopping of the energetic positrons. On the other hand, the low-temperature degradation at high field may be entirely due to the accumulation of ionization damage, in which case the electron and hole experiments would not show any effect. The curious fact that anthracene also exhibits a time-dependent degradation at low temperatures may possibly be connected with the more pronounced tendency of anthracene than perylene to strain upon cooling and thus to form "deep" trap states and additional scattering centers.

V. CONCLUSION

We have determined positron drift velocities u in a high-purity perylene single crystal as a function of applied electric field F and temperature by Doppler-shift measurements. The field-induced drift velocity displays a nonlinear field dependence at moderate fields with a characteristic velocity $v_s = 50$ km/s much greater than the longitudinal sound velocity in the solid. At high fields the drift velocity tends to saturate at a velocity $u_{\text{sat}} \simeq 110$ km/s. This saturation effect is presumably a consequence of optical-phonon generation when the positron field-induced kinetic energy exceeds the threshold energy necessary for optical-phonon generation. Over the temperature range 100–350 K, the mobility $\mu_{c'c'}$ exhibits a T^n temperature dependence with $n = -1.04 \pm 0.03$, showing a clear departure from the $T^{-3/2}$ dependence one might expect on the basis of the simplest theoretical model. Below 100 K, μ_0 decreases as the maximum applied field $F_{\max}$ increases, possibly indicating the presence of field-enhanced accumulation of trapped carriers that cause scattering at low temperatures. Taking the limit of μ_0 as $F_{\max} \to 0$, we find that the mobility below 50 K does not further increase beyond the fairly high value of $\mu = 1000$ cm^2 V^{-1} s^{-1}. In analogy to similar observations with electron and hole mobilities,[6,22] this fact is ascribed to the presence of residual impurities.

ACKNOWLEDGMENTS

The high-purity crystals were grown from extensively zone-refined material in the Kristallabor of the Physikalisches Institut at the University of Stuttgart, FRG; the technical assistance of Chr. Herb and W. Tuffentsammer is gratefully acknowledged.

[1] S. Berko and J. C. Erskine, Phys. Rev. Lett. **19**, 307 (1967).

[2] I. K. MacKenzie, T. L. Khoo, A. B. McDonald, and B. T. A. McKee, Phys. Rev. Lett. **19**, 946 (1967).

[3] See, for example, R. M. Nieminen, in *Positron Solid State Physics,* edited by W. Brandt and A. Dupasquier (North-Holland, Amsterdam, 1983), p. 359.

[4] N. Karl, J. Marktanner, R. Stehle, and W. Warta, Synth. Met. **41-43**, 2473 (1991).

[5] N. Karl, in *Crystals, Growth, Properties and Applications,* edited by H. C. Freyhardt (Springer-Verlag, Berlin, 1980), Vol. 4, pp. 1–100.

[6] N. Karl, J. Cryst. Growth **99**, 1009 (1990), Fig. 6.

[7] A. P. Mills, Jr., N. Karl, D. M. Zuckerman, J. Passner, J. Hensel, and C. D. Beling, Appl. Phys. A **54**, 22 (1992).

[8] A. P. Mills, Jr. and L. Pfeiffer, Phys. Rev. Lett. **36**, 1389 (1976). It is to be noted that in a noncubic single crystal, the drift velocity is not necessarily parallel to the applied field since the mobility is a tensor. We measure the component of the drift velocity in the given direction of the applied electric field, $u_{c'} = \mu_{c',c'} E_{c'}$ [cf. J. F. Nye, *Physical Properties of Crystals, their Representation by Tensors and Matrices* (Clarendon, Oxford, 1985)]. Moreover, the effective mass and the deformation potential are tensorial properties in noncubic crystals, and there are three different principal longitudinal sound velocities. For the sake of simplicity, we limit all discussions in the paper to a quasi-isotropic treatment.

[9] J. Bardeen and W. Shockley, Phys. Rev. **80**, 72 (1950).

[10] W. Shockley, Bell Syst. Tech. J. **30**, 990 (1951). For comments and references on the Druyvestyn model, see M. Sayed, K. O. Jensen, and A. B. Walker, Mater. Sci. Forum **105-110**, 811 (1992). Since we do not fit our data much beyond the characteristic velocity v_s, any inadequacies of Shockley model compared to the Druyvestyn model should have less than a 5% effect on our determinations of μ_0. It is not obvious which model is preferable, since we do not understand why v_s is so much greater than the longitudinal sound velocity.

[11] W. Warta and N. Karl, Phys. Rev. B **32**, 1172 (1985).

[12] P. Norton and H. Levinstein, Phys. Rev. B **6**, 478 (1972).

[13] E. J. Ryder and W. Shockley, Phys. Rev. **81**, 139 (1951).

[14] A. P. Mills, Jr., G. R. Brandes, D. M. Zuckerman, W. Liu, and S. Berko, Mater. Sci. Forum **105-110**, 763 (1992).

[15] A. P. Mills, Jr. and C. A. Murray, Appl. Phys. **21**, 323 (1980).

[16] A. P. Mills, Jr., E. M. Gullikson, L. Pfeiffer, and W. S. Rockward, Phys. Rev. B **33**, 7799 (1986).

[17] P. C. Jain, M. Eldrup, and J. N. Sherwood, in *Positron Annihilation,* edited by P. G. Coleman, S. C. Sharma, and L. M. Diana (North-Holland, Amsterdam, 1982), p. 674.

[18] According to I. K. Makenzie (unpublished), the positron mobility in Mylar is less than about 1 cm^2 V^{-1} s^{-1} and thus annihilations in the Mylar will make a negligible contribution to our signal.

[19] The positron lifetime in anthracene at 293 K is 325 ps according to Ref. 17. We assume that the lifetime in perylene is slightly shorter because of its higher density.

[20] R. D. Evans, *The Atomic Nucleus* (McGraw-Hill, New York, 1955), p. 628.

[21] N. Karl, in *Semiconductors,* edited by O. Madelung, M. Schulz, and H. Weiss, Landolt-Börnstein, New Series, Group III, Vol. 17i (Springer-Verlag, Berlin, 1985), pp. 106–218.

[22] N. Karl, in *Defect Control in Semiconductors,* edited by K. Sumino (Elsevier, Amsterdam, 1990), Vol. II, p. 1725.